Journal of
Materials Chemistry B

REVIEW

Cite this: J. Mater. Chem. B, 2017, 5, 4555

Biomedical applications of natural-based polymers combined with bioactive glass nanoparticles

Á. J. Leite [ab] and J. F. Mano *[abc]

Received 9th February 2017,
Accepted 10th May 2017

DOI: 10.1039/c7tb00404d

rsc.li/materials-b

In recent years, the combination of natural polymers with nanoparticles has permitted the development of sophisticated and efficient bioinspired constructs. In this regard, the incorporation of bioactive glass nanoparticles (BGNPs) confers a bioactive nature to these constructs, which can then induce the formation of a bone-like apatite layer upon immersion in a physiological environment. Moreover, the incorporation of bioactive glass nanoparticles has been found to be beneficial; the constructs proved to be biocompatible, promote cell adhesion and spreading, and regulate osteogenic commitment. This review provides a summary and discussion of the composition, design, and applications of bioinspired nanocomposite constructs based on BGNPs. Examples of nanocomposite systems will be highlighted with relevance to biomedical applications. It is expected that understanding the principles and the state-of-the-art of natural nanocomposites may lead to breakthroughs in many research areas, including tissue engineering and orthopaedic devices. The challenges regarding the future translation of these nanostructured composites into clinical use are also summarized.

Introduction

Bioactive glass-based materials are known for their bioactivity, which can be applied in various fields. From an orthopedic perspective, this bioactivity is due to a bonelike apatite layer that grows on the surface of the bioactive glass upon implantation.[3] This feature translates into acceptable anchorage to hard living tissues. Moreover, it prevents complications often related to implant failures, such as the formation of fibrous capsules, micromotion, and patient pain.[8]

However, this bioactivity also enables the release of ionic products, which affect cellular behavior. This characteristic means that bioglasses may have applications beyond orthopedics and be extended to the regeneration of other tissues, such as skin and cartilage.[11] Indeed, the angiogenic capacity of bioglasses in soft tissue is an example of this versatility.[12–14]

Researchers have also realized that the units of biological tissues have nanodimensions and that communications between cells and biomaterials occur on the nanoscale.[15–17] At this level, several interrelated properties regulate cell–biomaterial interactions, such as nanotopography, surface area and energy, hydrophilicity, and chemical composition.[18,19] These features govern contacts with proteins, modulating cell adhesion, spreading, and proliferation; finally, they affect the long-term functionality of implants.[17,20,21] Thus, in recent decades, nanotechnology has become a trending topic in tissue engineering; new bioactive nanomaterials with high potential for application are being developed and widely exploited.[23]

Nature has been inspiring scientists and engineers to mimic its highly functional biopolymeric systems.[25] In this regard, naturally derived polymers have been applied in biomedicine due to their biocompatibility, sustainability, and environment-friendly chemistry.[28] Currently, rapid technological advances are permitting the combination of nanoscale bioactive glasses with natural polymers, allowing the design and build of various nanostructured biocomposites for biomedical purposes. These applications include tissue-engineered scaffolds, site-specific drug delivery systems, non-viral gene carriers, biosensors, screening, and clinical diagnostics systems.

This review will describe the main features of bioactive glass nanoparticles and provide a brief description of their methods of production. Further, we will focus on nanocomposites constituted from natural polymers and bioactive glass nanoparticles, addressing the state-of-the-art technologies and their applications. A final summary prospecting the areas of future research will also be provided.

Bioactive glass nanoparticles

Bioactive glass nanoparticles (BGNPs) are usually composed of silicates or phosphosilicates combined with distinct proportions

[a] 3B's Research Group – Biomaterials, Biodegradables and Biomimetics, University of Minho, Headquarters of the European Institute of Excellence of Tissue Engineering and Regenerative Medicine, Avepark – Parque de Ciência e Tecnologia, Zona Industrial da Gandra, 4805-017 Barco, Guimarães, Portugal
[b] ICVS/3B's – PT Government Associate Laboratory, Braga/Guimarães, Portugal
[c] Department of Chemistry, CICECO, University of Aveiro, 3810-193 Aveiro, Portugal. E-mail: jmano@ua.pt

of glass modifiers, such as sodium oxide (Na_2O) and calcium oxide (CaO). As bioactive glasses, they show high bioactivity and excellent bone bonding properties. The conventional compositions are binary, ternary, or quaternary systems, such as SiO_2–CaO, SiO_2–CaO–P_2O_5, and SiO_2–CaO–P_2O_5–Na_2O, respectively.[29,30]

Production methods

BGNPs can be produced by various techniques, such as microemulsion, flame synthesis, and sol–gel.[31] A summary of the compositions and sizes of BGNPs produced by various methods are present in Table 1.

Flame spray. In this process, a nozzle forms an oxygen spray that disperses the metal–organic precursors present in a liquid mixture.[2,31–33] The spray is ignited; as it burns at temperatures above 1000 °C, the organic constituents of the liquid precursor combust to water and carbon dioxide while the metal constituents oxidize to form the nanoparticles. The gas-phase synthesis method forms molecular nuclei followed by condensation and coalescence, inducing the growth of nanoparticles in high-temperature regions during the process.[2,31–33] The main factor affecting particle size is the mean residence time of the particles in the high-temperature regions. High cooling rates (>1000 K s^{-1}) and residence times (± 1 ms) enable the formation of nanoparticles (Fig. 1A). The process can produce various nanoparticles with distinct compositions and with high chemical homogeneity.[2,31–33]

Microemulsion. In water-in-oil microemulsions, the hydrocarbon phase scatters nanosized water droplets, usually between 5 and 20 nm, which become surrounded by a monolayer of surfactant molecules. These aqueous droplets act as minuscule reactors where reactions take place when droplets containing the reactants collide. An example of this method is the formation of precursor particles of hydroxide or oxalate in a microemulsion system. The desired oxide system is then developed after drying

Table 1 Composition and size of BGNPs produced by different techniques

Technique	Configuration	Size (nm)	Composition (wt%)
Sol–gel	SiO_2–CaO	40	70 : 30[40]
		50–90	75 : 25[84]
		100	70 : 30[36]
	SiO_2–CaO	300	70 : 30[29]
	SiO_2–CaO–P_2O_5	24	62.1 : 28.5 : 9.2[85]
		30	58 : 33 : 9[11]
		30	80 : 15 : 5[11]
		50	70 : 25 : 5[72]
		50	64 : 31 : 5[72]
		70	6.3 : 71 : 22.7[59]
		87	60 : 36 : 4[86]
		75–37	45 : 40 : 5[55]
		10–100	58 : 33 : 9[54]
		30–100	66 : 27 : 7[38]
		100	58 : 35 : 7[87]
		100	62 : 30 : 9[88]
		100	79 : 19 : 2[48]
		100	35.4 : 57.4 : 7.2[87]
		100	62.2 : 28.5 : 9.2[88]
		300	60 : 36 : 4[29]
		500	58 : 33 : 9[53]
	SiO_2–CaO–P_2O_5–Ag_2O	79	50 : 35 : 5 : 10[73]
		100	56 : 30 : 3 : 10[89]
		100	58 : 23 : 9 : 10[74]
	SiO_2–CaO–P_2O_5–CuO	87	50 : 35 : 5 : 10[73]
	SiO_2–CaO–P_2O_5–MgO	30–60	64 : 26 : 5 : 5[90]
	SiO_2–CaO–P_2O_5–Na_2O	100	45 : 24.5 : 24.5 : 6[91]
	SiO_2–CaO–P_2O_5–Na_2O	300	46.1 : 26.9 : 2.6 : 42.4[29]
	SiO_2–CaO–P_2O_5–SrO	50	55 : 30 : 5 : 10[92]
	SiO_2–CaO–P_2O_5–TiO_2	50	55 : 35 : 9 : 1[76]
	SiO_2–CaO–SrO	80–100	84 : 5 : 11[93]
	SiO_2–CaO–ZnO	80–90	85 : 10 : 5[79]
Flame	SiO_2–CaO–Na_2O	20–80	74.3 : 11.8 : 14[2]
	SiO_2–CaO–Na_2O–B_2O_3	20–80	58.7 : 20.4 : 12.8 : 8.1[2]
	SiO_2–CaO–P_2O_5	20–80	79.9 : 16.8 : 3.2[2]
	SiO_2–CaO–P_2O_5–Na_2O	20–50	44.7 : 27.6 : 4.9 : 22.8[49]
		20–60	44 : 24.5 : 24.5 : 7[94]
		20–80	47.8 : 25.1 : 22.6 : 4.6[2]
	SiO_2–CaO–P_2O_5–Na_2O–K_2O–MgO	30	53 : 20 : 4 : 6 : 12 : 5[81]
	SiO_2–CaO–P_2O_5–Na_2O–K_2O–MgO–SrO	30	53 : 15 : 4 : 6 : 12 : 5 : 5[81]
	SiO_2–CaO–P_2O_5–Na_2O–F	20–80	45.4 : 26.6 : 4.3 : 21.4 : 2.4[2]
Microemulsion	SiO_2–CaO–P_2O_5	10–40	60 : 36 : 4[7]
	SiO_2–CaO–P_2O_5	100	21 : 60 : 19[95]

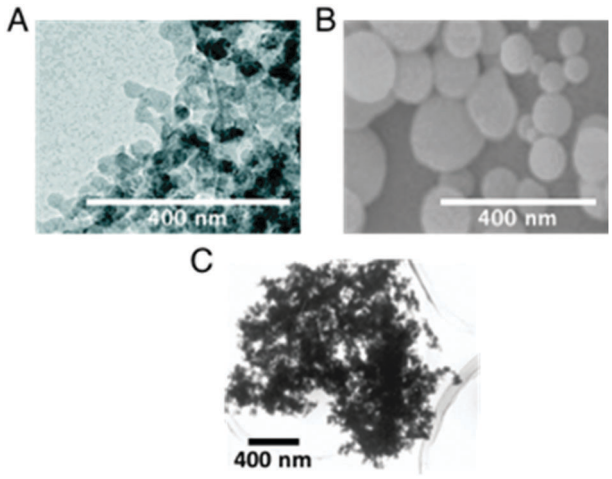

Fig. 1 Morphologies of BGNPs produced by different methods. (A) TEM image of a flame-made BGNP sample showing a high degree of agglomeration (SiO_2–CaO–P_2O_5–Na_2O). (B) SEM images of BGNPs generated by microemulsion (SiO_2–CaO–P_2O_5). (C) TEM micrograph of BGNPs produced by the sol–gel process (SiO_2–CaO–P_2O_5). Adapted from ref. 2, 7 and 9, respectively.

and calcination of the precursor powder at a defined temperature (Fig. 1B). Microemulsion techniques can achieve nanoscale particles with low agglomeration. However, the main disadvantages of the microemulsion technique are the production yield and the use of large amounts of oil and surfactants.[7]

Sol–gel. The common sol–gel technique for BGNP production is an adapted procedure of the Stöber method.[34] In this approach, the glass compositional precursors are first hydrolyzed to a sol under acidic conditions and then condensed and precipitated to gel particles in alkaline solution. A common silicate precursor is tetraethylorthosilicate (TEOS), while the calcium precursors are calcium nitrate or calcium chloride and the phosphate precursors are triethylphosphate or diammonium hydrogen phosphate. Briefly, the procedure starts with hydrolysis of TEOS in water or a water/alcohol acidic mixture (creating Si–OH groups). Then, the addition of a base (usually ammonia) allows condensation through the release of water molecules and the formation of Si–O–Si bonds, forming a colloidal sol. In this stage, calcium acts as a modifier as it is ionically bonded to the silicon *via* non-bridging oxygen bonds (Si–O–Ca). Also, when phosphorus is incorporated into the BGNP formulation, it forms orthophosphates, which are charge balanced by calcium ions.[35,36] The primary nanoparticles present in the sol coalesce and bond together, forming a silica-based gel network of assembled nanoparticles. This gelation step continues from minutes to a few hours after adding pre-hydrolyzed TEOS to the basic solution. A further drying step is used to remove excess water and prevent secondary aggregation of the gel particles by linkage with water molecules. The gel network is broken by calcination at a temperature above 680 °C. This process also stabilizes the incorporation of calcium and phosphorous (when applicable) and removes nitrates and organic phases. Finally, BGNPs are obtained (Fig. 1C). Experimental conditions such as pH, solvent volumes, reagent ratios and surfactants can be changed. This milieu influences the processes of hydrolysis and condensation and determines the chemical composition, agglomeration, and size of the BGNPs. Also, the synthesis and calcination temperature has an important effect on the crystallization process of BGNPs. The sol–gel route allows easier control of the chemical composition, morphology, size, and structure.[9,13,37–43] In a variation of the method, Liang *et al.* synthesized two types of mesoporous BGNPs using a sacrificial liquid template by a sol–gel method. They produced spherical nanoparticles with radial mesoporous and pineal nanoparticles with lamellar mesopores.[44] With this methodology, the size and structure of the nanoparticles could be tuned by the reaction conditions. Lei *et al.* also developed BGNPs with controllable sizes and morphologies by combining an acid-catalyzed sol–gel process and gelation-induced phase separation technology.[45] These findings demonstrate the effects of BGNP production methods on their physicochemical and biological properties.

Physiochemical properties and biological implications

Size and surface area. Particle size and surface area play a significant role in the interaction of materials with cells. As mentioned, nanomaterials have a high surface area to volume ratio.[46] For example, Gerhardt *et al.* described microsized Bioglass® with a median particle size of 4.3 μm and a specific surface area of 2.7 $m^2\ g^{-1}$; nanoscaled Bioglass®, with diameters of 35 to 40 nm, presented a specific surface area of 79 $m^2\ g^{-1}$.[47] This feature confers a higher surface energy and surface reactivity to nanoscale bioactive glasses when compared with their microscale counterparts. Thus, a nanoscale bioactive glass holds a faster ion release rate and an increased surface area for protein adsorption. As a result, these nanoparticles can promote cell adhesion, proliferation, and differentiation.[21,48–51] The size of bioactive glasses has shown to affect their *in vitro* osteogenic capacity.[52,53] Caridade *et al.* also found that Bioglass® nanoparticles induced early precipitation of apatite in SBF compared with microsized Bioglass®.[52,53] In fact, compared with microsized particles, Bioglass® glass nanoparticles promoted higher adhesion of human osteoblast-like cells (MG-63) and induced an early and superior osteogenic gene expression of alkaline phosphatase (ALP), runt-related transcription factor two (RUNX2) and collagen I (COL1).[53] Gong *et al.* reported similar results with a distinct composition of the nanoscale bioactive glass.[54] The authors found that the ionic dissolution of BGNPs improved cell proliferation and activation of osteogenic genes when compared with micro bioactive glasses.[54] These studies showed that BGNPs have a higher ability for apatite formation and stronger osteogenic ability compared with microscale bioactive glasses. Even inside the nanolimits, distinct sizes lead to distinct results. Ajita *et al.* compared three sizes of nano bioactive glasses (approx. 74.7 nm, 43.25 nm, and 37 nm) in mouse mesenchymal stem cell behavior.[55] They showed that all the BGNPs were non-cytotoxic at 20 mg mL^{-1} but noted increased proliferation in cells treated with the smallest nanoparticles.[55] Additionally, the dissolution rates of ions varied according to the size of the nanoparticles. Also, the particles with smaller sizes triggered lasting activation of extracellular regulated kinases and

upregulation of cyclin genes that modulate the cell cycle from the G0/G1 phase to the S and G2/M phases.[55] This study highlighted the dependency of the cell proliferative action on nano-sized particles.

Morphology. It is also important to understand the relationship between the size and shape of particles to develop effective nanomaterials. The majority of the produced BGNPs presented spherical shapes. Indeed, it has been reported that endocytosis of spherical nanoparticles is easier and faster compared to that of rod-shaped or fiber like nanoparticles.[56,57] However, non-spherical nanoparticles may be advantageous in certain applications. These nanoparticles can be combined with natural polymers to design bioactive biomaterials with improved mechanical properties.[58] In this regard, Hong *et al.* synthesized rice-shaped BGNPs.[59] *In vitro* bioactivity tests showed that these novel bioactive nanoparticles have excellent biomineralization capability.[59] Other studies also reported the production of BGNPs with distinctive shapes that ranged from pineal and spherical to short and long rods.[44,60] This shapes may be biologically advantageous in biomaterials, as natural bone materials contain micro/nanoscale needles or rod-like hydroxyapatite structural units.[61]

Surface properties. The surface of BGNPs largely defines their performance in biological systems. Various aspects, such as selective protein adsorption and transmembrane permeability, are regulated by the surface of nanoparticles. Surface charge is a determinant in the aggregation of nanoparticles. Bearing this in mind, Chen *et al.* improved the dispersibility of BGNPs by coupling a silane agent onto the surface of the nanoparticles. The results indicated that $-NH_2$ groups appeared on the surface of the modified BGNPs, proving that the groups of the silane agent were covalently bonded to the surface of the BGNPs.[62] In another study, Lee *et al.* investigated the uptake efficiency of amine-functionalized BGNPs and their role in odontogenic differentiation.[63] BGNPs were fabricated by sol–gel synthesis, and a silane agent was used for surface functionalization, changing the charge of the nanoparticles from negative to positive. The uptake of amine-functionalized BGNPs in rat dental pulp stem cells was determined to be about 92% after 4 hours of incubation. The results also indicated that amine-functionalized BGNPs induce odontogenic differentiation, as the expression of odontogenic-related genes (BSP, COL1A, DMP-1, DSPP, and OCN) and the capacity for biomineralization were significantly upregulated.[63]

Porosity. Factors such as porosity can empower the function of nanoparticles. Indeed, development of porous BGNPs for drug delivery applications is increasing.[64] The porosity, pore size, and pore shape of BGNPs can be controlled by tuning the previously described production methods through the use of templates (*i.e.* CTAB and CPB).[44,65] The resulting porous or hollow structures of BGNPs can provide larger specific surface areas and voids, which may be useful as containers for drug delivery applications.[66] In this regard, Kim *et al.* studied the potential of BGNPs for gene delivery of mesenchymal stem cells (MSCs).[67] The BGNPs were designed with enlarged pore sizes to efficiently load and deliver bone morphogenetic protein-2 (BMP2) and plasmid DNA (BMP2–pDNA). Moreover, the BGNPs were efficient in the loading and in the sustained release of BMP2–pDNA. The BMP2–pDNA/BGNPs complexes were internalized in MSCs, and the majority of cells were transfected to express the BMP2 protein.[67]

Composition. The chemical nature of BGNPs also contributes to the role of the nanoparticles. Indeed, the porous structure and surface area of the BGNPs were shown to be dependent on their composition.[68] In this regard, the composition of BGNPs affects the ability of the material to support the proliferation and function of cells.[69–71] Moorthi *et al.* synthesized ternary BGNPs (SiO_2–CaO–P_2O_5) with different amounts of calcium oxide and silica (70 : 25 : 5 and 64 : 31 : 5 mol%) and studied their role in osteoblast proliferation.[72] Both BGNPs were non-cytotoxic to MG-63 cells; however, the formulation with higher calcium content was more effective in osteoblast proliferation and promoted cell proliferation, with more cells entering into G2/M cell cycle phases. Also, they observed a clear expression of cyclin proteins.[72] These results suggest that adapting the ionic constituents of BGNPs can lead to distinct biological properties. It is estimated that the controlled release of ions from bioactive glasses can stimulate interactions with tissues, such as new bone growth.[69] The rate of ion release depends primarily on the composition, particle size and surface area, which affect osteogenesis and angiogenesis. In this regard, BGNPs became a vehicle for the local delivery of specific ions to control cellular functions. Ion-doped BGNPs are being designed for the controlled release of specific metal ions, which can increase osteoblast activity (for example, in strontium doped-BGNPs) or have valuable anti-inflammatory effects (for example, in zinc-doped BGNPs). Copper-doped BGNPs (SiO_2–CaO–P_2O_5–CuO) and silver-doped BGNPs (SiO_2–CaO–P_2O_5–Ag_2O) have antibacterial properties, preventing bacterial colonization.[73–75] Goh *et al.* described the ion release profiles of these BGNPs. The authors noted a faster release of Ag, which made silver-doped BGNPs a rapid bacteria-killing agent. Meanwhile, because of their slower release, copper-doped BGNPs may be suitable candidates for long-term antibacterial protection.[73] Copper-doped BGNPs have also been synthesized to decrease or inhibit the growth of pathogens. The authors concluded that the nanoparticles showed bioactive behavior with antimicrobial activity against *Staphylococcus aureus* as the copper content increased.[75] Also, titanium dioxide can be a powerful antibacterial substance, as TiO_2 shows high oxidizing power under irradiation with UV light. Therefore, Rajendran *et al.* prepared titanium-doped BGNPs (SiO_2–CaO–P_2O_5–TiO_2).[76] They reported antibacterial effects against *Escherichia coli* and *Staphylococcus aureus*. Additionally, cytotoxicity tests showed that the nanoparticles were non-cytotoxic and showed improved cell viability in MG-63 cells at a concentration of 125 μg mL^{-1}.[76] These particles could thus reduce bacterial infections in biomaterial implants. Zinc-doped BGNPs (SiO_2–CaO–ZnO) were shown to promote odontogenic differentiation and angiogenesis. The zinc ion is an essential trace element in bone and is considered for use in osteoporosis treatments.[77,78] Zhang *et al.* tested zinc-doped BGNPs on human dental pulp cells.[79] The zinc-doped BGNPs increased ALP activity,

improved the formation of mineralized nodules, and upregulated mRNA expression of odontogenic differentiation marker genes in a time and dose-dependent manner.[79] Strontium-doped BGNPs showed favorable effects on osteogenic stimulation and bone formation. In this regard, Strobel *et al.* assessed the osteogenic potential of BGNPs containing strontium (SiO_2–CaO–P_2O_5–Na_2O–K_2O–MgO–SrO) on human bone marrow stromal cells (hBMSCs).[80] Cell growth and morphology studies showed the high cytocompatibility of the nanoparticulate bioactive glass. Moreover, the strontium-doped particles improved the expression of osteocalcin, collagen type I and vascular endothelial growth factor.[80] However, is also important to notice that increasing their strontium content can delay the bioactive behavior of BGNPs because of the inhibitory effect of strontium on apatite mineralization.[81] Xue *et al.* synthesized monodispersed europium (Eu)-doped BGNPs with a dual function of bioactivity and luminescence by a template-assisted sol–gel method. The fluorescence was achieved by doping Eu into the BGNP network, which did not decrease their biomineralization potential. The nanoparticles also demonstrated cellular biocompatibility by enhancing the proliferation and metabolic activity of osteoblast cells. Also, BGN–Eu was successfully used to label a mouse osteoblastic cell line (MC3T3) by strong red fluorescence with low background noise.[82]

Nanoparticle safety

The safety of nanoscale particles is an issue of concern. Although studies have shown that nanoscale bioactive glass show equal performance compared to commercial micropowder bioactive glasses, this topic will also be considered in this review.

Despite the acceptable non-cytotoxicity and non-genotoxicity of BGNPs, concerns have arisen about their internalization from cells and the resulting long-term body biodistribution. It is known that a localized increase in intracellular silica and calcium concentrations can have a marked effect on cell metabolism or inflammatory response. Another concern is that if the particles dissolve intracellularly, they may also break up into finer particles that can escape the endosomal pathway and enter the cell cytoplasm or even the nucleus. In this regard, studies have addressed the issue by studying the response of MSCs and adipose tissue-derived stem cells (ADSCs) to BGNPs.[42,83] The results confirmed cellular uptake and localization of the nanoparticles in the cell cytoplasm and cell endosomes and partial particle dissolution inside the cells. It was hypothesized that the dispersion of particles, combined with a finer control of their size, dramatically increased the number of particles taken up by the cells. However, the uptake mechanism remained unclear.

More importantly, the particles were non-cytotoxic at lower concentrations and had slight effects on the viability of primary MSCs and ADSCs at higher concentrations (100 and 200 μg mL^{-1}). Also, BGNPs had negligible effects on cell proliferation compared with the control.

These slight effects on cell metabolism and proliferation combined with the large numbers of particles detected inside the cells showed acceptable safety. Also, these results pave the way for the use of BGNPs as injectable target particles to be internalized by cells for the continuous local delivery of inorganic therapeutic ions.[42,83]

Nanocomposites

The development of composite materials is an attractive field in tissue engineering. The favorable properties of two or more types of materials can be combined to tailor the response of a biomaterial to the mechanical and physiological demands of the host tissue.

Specifically, in bone tissue engineering, the bioactivity of a biomaterial is an important feature. However, several attractive biomaterials are not intrinsically bioactive.[96] A strategy to provoke desirable bioactive behavior is the inclusion of nanoscale bioactive glasses in the polymer matrix, creating a composite material. The volume fraction of nanoscale bioactive glasses can adjust the bioactivity of the resulting composite while retaining the properties of the polymer, such as the ability to deform under loads.[97,98] This combination has already been used to create nanocomposite materials for orthopedic implants, bone filler materials, injectable bone materials, 3D biocompatible scaffolds, and membranes (Fig. 2).[9,97–101]

Despite their bioactive benefits, other general properties should be noted when polymer matrices incorporate BGNPs.

Mechanical properties

It is known that nanoscale bioactive glasses can cause significant improvements in the mechanical properties of composite scaffolds, namely their elastic moduli and, for strong interfacial bonding, their tensile compressive strengths.[9,18,70,96,102–104] Furthermore, this feature results in a synergistic gain.

In one way, combination with polymers overcomes the lack of cohesive strength of the particulate BGNPs and prevents their possible displacement and migration under externally applied forces during the healing period.[105] Therefore, BGNPs are incorporated within polymeric systems, where the polymer acts as a continuous medium for immobilization of the particles.

In another way, the nanosize of BGNPs strengthens the polymers. As previously stated, because of the greater specific surface area, the nanofiller will enable higher contact effects. This feature results in improved mechanical properties of the materials when compared with micrometer-structured composites.[52] Also, strategies to prevent the agglomeration of the nanoscale reinforcements enable fine homogeneous dispersion of the nanofillers in the polymer matrix, which also contributes to strengthened mechanical properties.[9,100,106]

Degradation properties

The addition of nanoscale bioactive glasses to bioresorbable polymers can alter the polymer degradation rate. This outcome occurs because of the rapid exchange of protons in water for the alkali elements of the bioactive glass. The resulting change in the surface and bulk properties of the composites increases the hydrophilicity and water absorption of the polymer matrix,

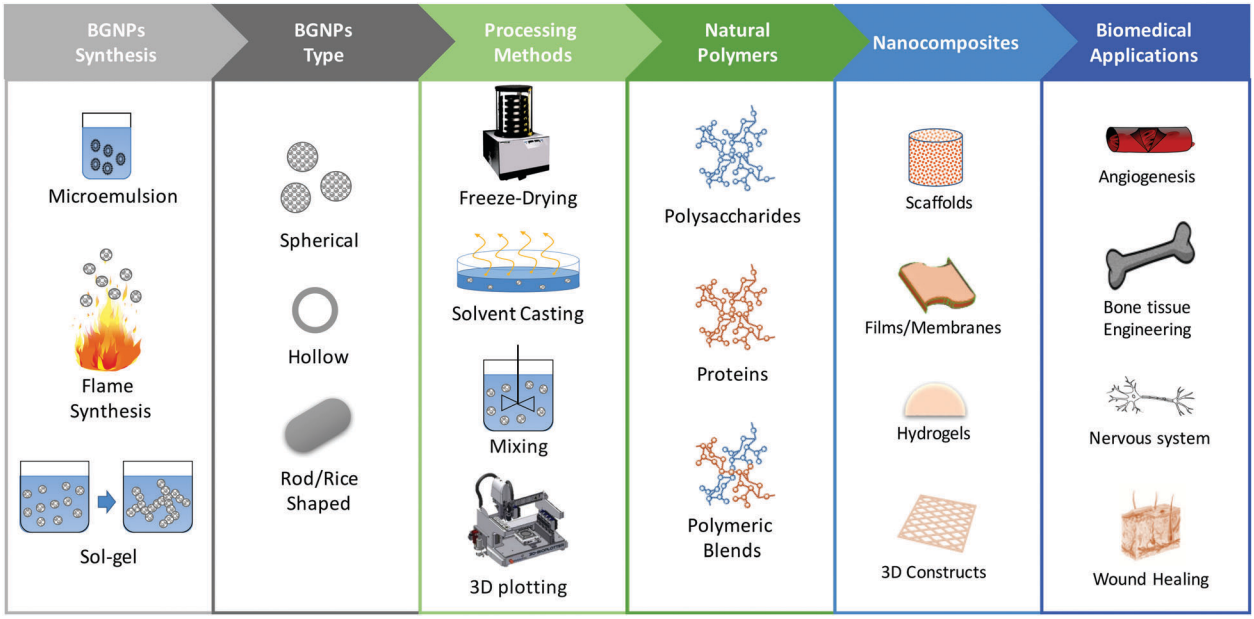

Fig. 2 Naturally derived nanocomposites: from the production of bioactive glass nanoparticles to their biomedical applications.

which alters the scaffold degradation kinetics.[102,107] Also, bioactive glasses can produce an alkaline environment.[108] Thus, when a composite incorporates BGNPs, this increase in pH can prevent the acidic degradation of some polymers. However, this alkalization can also affect the functionality of the composite. For instance, studies on dental applications showed that the increase in pH caused by BGNPs could buffer the acidity induced by polymeric scaffolds, which contributed to lower antimicrobial activity and thus canceled its therapeutic effects.[109] It can be assumed that even if occasionally useful, the buffering effect of BGNPs in this dental application was deleterious to its final application.

This finding clearly showed that the biomaterial design must be adapted to the targeted role.

Biological properties

Regarding their biological properties, BGNPs can create nanostructured features in composites as nanotopographies on the scaffold surface. This characteristic may increase contact effects, which can also contribute to improved bioactivity.[110]

Thus, incorporating nanoparticles in biopolymers can modulate protein absorption. This surface tailoring may improve cell attachment and the resulting cell behavior.[96] In fact, the higher surface area increases the interactions between the surface of an implant and its biological environment.[111]

Also, in bone applications, the insertion of nanoparticles into a polymeric matrix is thought to mimic the nanocomposite-like bone structure. Webster *et al.* have reported a significant increase in protein adsorption and osteoblast adhesion on nanoscale ceramic materials compared with micron-sized ceramic materials.[112] Also, mimicking the nanoscale features of bone at the surface of synthetic bone implants has been shown to increase cell adhesion, proliferation, and bone formation.[51] Also, the extracellular matrix (ECM), which surrounds cells in their natural environment, is a nano-organized structure formed by biomolecules configured in distinct geometric arrangements.[113,114]

Natural polymers in nanocomposites

Naturally derived polymers have been widely proposed for use in tissue regeneration because they are similar to macromolecules present in the biological environment and produce degradation products that can be recognized and metabolized by the body.[28] A summary of nanocomposite constructs based on BGNPs and natural polymers is provided in Table 2.

Alginate

Alginate is a natural polysaccharide obtained from brown seaweeds that form stable hydrogels in the presence of divalent cations. It is hydrophilic, biocompatible, and inexpensive and is commonly employed in the food and pharmaceutical industries.[115,116]

Srinivasan *et al.* tested the impact of BGNPs on alginate for periodontal tissue regeneration by producing composite scaffolds by freeze-drying (Fig. 3A).[1] The results showed reduced swelling, which may be due to the strong binding between alginate and BGNPs and to the decrease in pore size. Also, the exposed BGNPs on the scaffold surfaces increased the binding sites on the surface, which may be responsible for the improved biomineralization and protein adsorption observed by the authors. Additionally, BGNPs encouraged the attachment and proliferation of human periodontal ligament fibroblast (hPDLF) and MG-63 cells. This effect was also ascribed to the increases in surface area and surface roughness because of the incorporation of BGNPs. The presence of BGNPs improved the ALP activity of hPDLF cells with a ceiling of seven days because of the release of

Table 2 Summary of polymeric nanocomposites based on bioactive glass nanoparticles and natural polymers

Polymer(s)	BGNPs	Structure	Production technique	Applications
Alginate	SiO_2–CaO–P_2O_5	Scaffold	Freeze drying	Periodontal tissue regeneration[1]
Alginate/gelatin	SiO_2–CaO–P_2O_5–Na_2O	Films	Casting	Bone tissue engineering[141]
Alginate dialdehyde–gelatin	SiO_2–CaO–P_2O_5	Construct	Bioplotting	Bone tissue engineering[92]
Chitin	SiO_2–CaO–P_2O_5	Scaffold	Freeze drying	Bone tissue engineering[4]
Chitosan	SiO_2–CaO	Membrane	Solvent casting	Guided tissue regeneration[40,99]
	SiO_2–CaO–P_2O_5	Films	Layer by layer	Coatings of orthopedic implants[142]
		Hydrogel	Mixing	Bone tissue engineering[5]
			Mixing	Injectable systems[101]
		Membrane	Solvent casting	Guided tissue regeneration[127]
			Stamping	Patterned medical membranes[128]
		Scaffold	Freeze drying	Bone tissue engineering[132]
	SiO_2–CaO–P_2O_5–MgO	Membrane	Solvent casting	Bone tissue engineering[90]
Chitosan/hyaluronic acid	SiO_2–CaO–P_2O_5	Films	Layer by layer	Coatings of orthopedic implants[143]
		Membrane	Layer by layer	Guided tissue regeneration[144]
	SiO_2–CaO–P_2O_5–Ag_2O	Films	Layer by layer	Antibacterial coatings for orthopedic implants[89]
Collagen	SiO_2–CaO–P_2O_5	Membrane	Electrospinning	Bone regeneration[145]
	SiO_2–CaO–P_2O_5–Na_2O	Films	Compression molding	Angiogenic properties[10]
Collagen/hyaluronic acid/ phosphatidylserine	SiO_2–CaO–P_2O_5	Scaffold	Freeze drying	Bone tissue engineering[27,146]
Gelatin	SiO_2–CaO–P_2O_5	Scaffold	Freeze drying	Nerve regeneration[22]
				Bone tissue engineering implants[137]
Gelatin/chitosan	SiO_2–CaO–P_2O_5	Scaffold	Freeze drying	Alveolar bone regeneration[140]
Gelatin/collagen	SiO_2–CaO–P_2O_5–Na_2O	Scaffold	Freeze drying	Myocardial regeneration[147]
Gellan gum	SiO_2–CaO	Scaffold	Freeze drying	Bone tissue engineering[24]

ions and dissolution products from the bioactive glass accompanied by a subsequent decline of this expression. The decrease after seven days can be assigned to the culmination of osteoblastic differentiation.[1] Therefore, the results indicate that these biocompatible composite scaffolds could be advantageous for periodontal tissue regeneration.

Several researchers developed nanocomposite films and scaffolds which combined alginate with BGNPs and were cross-linked with Cu^{2+}, Ca^{2+}, and Ga^{3+} for bone tissue engineering.[117–120] The incorporation of BGNPs into alginate significantly improved the tensile strength of the nanocomposites.[117–119] Biomineralization studies indicated the deposition of apatite on the surface of the films, suggesting their bioactive behavior as a consequence of the added BGNPs.[117–119] The *in vitro* results indicated that the bioactive ions released from both nanocomposite biomaterials stimulated the differentiation of rat bone marrow-derived mesenchymal stem cells (rBMSCs) towards the osteogenic lineage.[118] The typical endothelial cell property of forming tubes in Matrigel was observed for human umbilical vein endothelial cells (HUVECs) when in contact with the biomaterials, which indicates their angiogenic properties.[118] Ga–alginate films containing BGNPs induced a bacteriostatic effect *in vitro* towards *S. aureus* due to the presence of Ga^{3+} ions.[119]

Chitin

Chitin is a harmless and biodegradable polymer that is structurally analogous to the ECM of many physiological tissues. Due to these features, chitin is an interesting material to consider for several biomedical applications.[121,122] The lack of solubility of chitin in most solvents is a challenge to the use of polysaccharide in the fabrication of devices. However, it is possible to fabricate nanocomposite scaffolds that combine chitin with BGNPs by a freeze-drying procedure (Fig. 3B).[4,123] Chitin was first added to a mixture of $CaCl_2{\cdot}2H_2O$/methanol and mixed until a clear solution was achieved. Then, the undissolved chitin was separated by filtration and dialyzed to extract the calcium ions. The chitin hydrogel was blended with BGNPs and freeze-dried to obtain the composite scaffolds. The resulting scaffolds showed a homogeneous dispersion of BGNPs on their porous surfaces. Further, the scaffolds showed increased swelling, bioactivity, and degradation compared to the control scaffolds without BGNPs. The composite scaffolds were non-toxic to MG-63 and human primary osteoblast (hPOB) cells and sustained cell attachment, spreading, and proliferation. Mineralized bone nodules and calcium precipitates also formed, showing strong mineralization of the hPOB cells. The development and mineralization of the hPOB cells without osteogenic

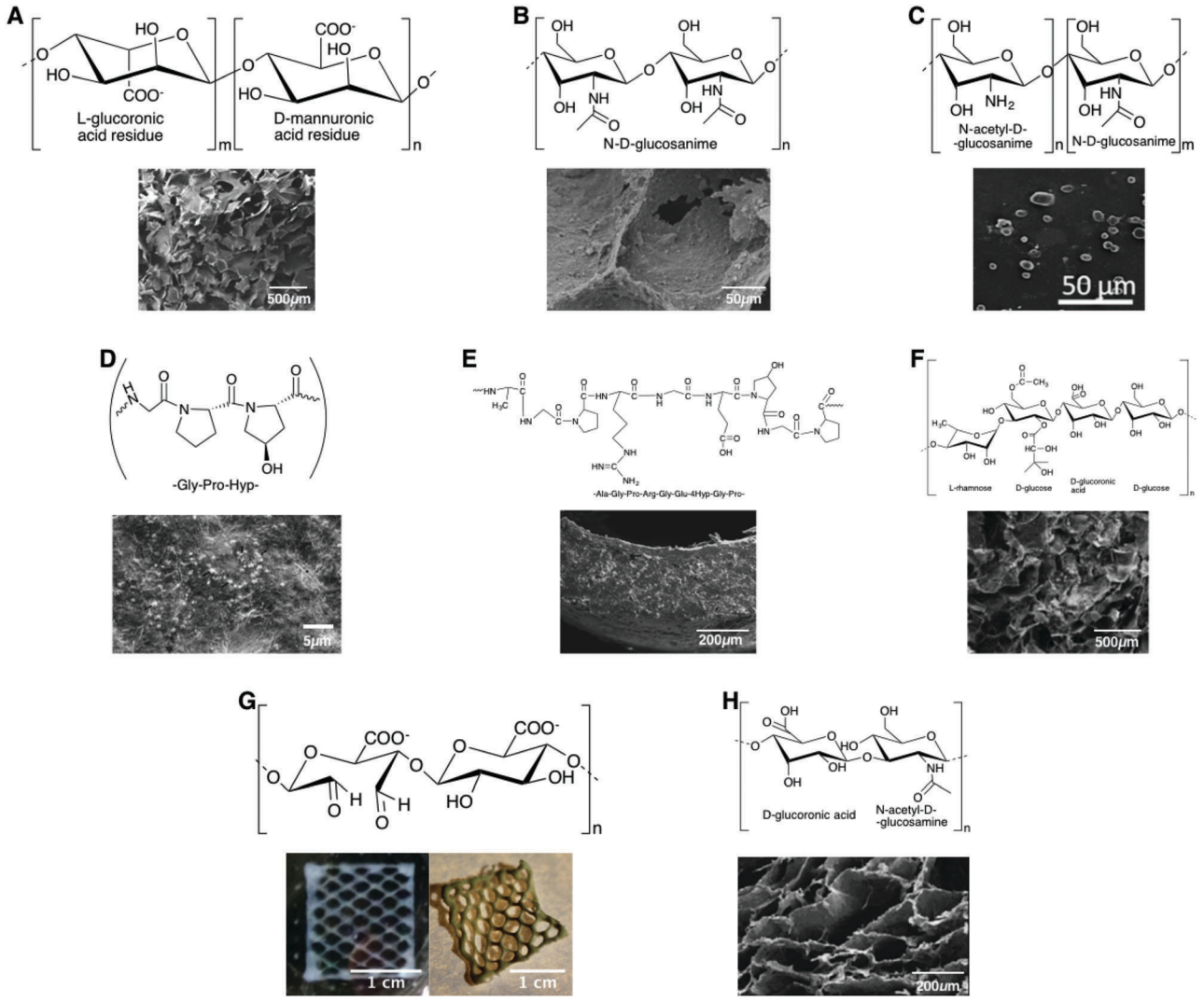

Fig. 3 (A) Structure of alginate polymer and SEM image showing the macroporous construct of the alginate/BGNPs composite scaffold; adapted from Srinivasan *et al.*[1] (B) The structure of chitin polymer and SEM images of the macroporous structure of the composite scaffolds. The pore sizes ranged from 150 to 500 μm; adapted from Peter *et al.*[4] (C) Structure of chitosan polymer and SEM micrograph of MC3T3-E1 response after three days of cell culture; adapted from Oliveira *et al.*[5] (D) Fragment structure of collagen type I, where ProHypGly is the most common triplet,[6] and the microstructure of 20 wt% BGNPs containing collagen film. Note the micron-sized clusters of BGNP particles (arrows); adapted from Vargas *et al.*[10] (E) Cross-section from the porous gelatin nanocomposite conduit; adapted from Koudehi *et al.*[22] (F) Structure of gellan gum polymer and SEM images of the scaffolds with 50 wt% of BGNPs; adapted from Gantar *et al.*[24] (G) Structure of alginate–dialdehyde polymer and figures depicting the fabricated constructs of ADA–GEL–BGNPs in hydrated and dehydrated forms; adapted from Leite *et al.*[26] (H) Structure of hyaluronic acid polymer and SEM micrographs of composite scaffolds prepared from cross-linked BGNPs–COL–HYA–PS; adapted from Wang *et al.*[27]

supplements confirmed the desirable features of the nanocomposites.[123] These nanocomposite scaffolds are potential contenders for tissue engineering purposes.

Chitosan

Chitosan (CHT) is a biopolymer produced from the deacetylation of chitin; it is soluble in aqueous acid solutions, which offers high processability.[124,125] CHT is biocompatible, biodegradable to innocuous products and non-antigenic.[28,126] Therefore, CHT has been extensively used for biomedical studies.

To improve the bioactivity and mechanical properties of CHT-based structures, nanocomposites that combine CHT and BGNPs are also being studied. In this regard, Couto *et al.* combined a CHT–glycerophosphate salt formulation with BGNPs to produce bioactive thermo-sensitive hydrogels.[101] The system gelled at around 36.8 °C, which is applicable for intracorporeal purposes. The hydrogel proved to be bioactive, and the density of the apatite deposits increased with the addition of BGNPs. This system may be used as a thermo-sensitive hydrogel for orthopedic rehabilitation as the nanosize of the BGNPs guaranteed the efficient injection of the nanocomposite into bone defects through small-gauge needles.[101] A high-throughput screening of hydrogel nanocomposites was developed to select the leading combination that influences the pre-osteoblast response.[5] The addition of BGNPs in quantities greater than 12.5% (wt/wt of CHT) considerably improved the storage modulus of the hydrogels.

The elastic modulus determined for this formulation also fits the values described for the granulation tissue occurring during bone regeneration. Moreover, this amount of BGNPs favored MC3T3 pre-osteoblast cell proliferation and spreading (Fig. 3C).[5]

CHT was also combined with distinct formulations of BGNPs, ternary nanoparticles and magnesium-doped BGNPs, to produce membranes for guided tissue regeneration.[90,99] These membranes were employed as boundaries to limit faster-growing soft tissue cells at the injury site and to restore periodontal ligaments, cementum, or bone.[90,99,127] These nanocomposite membranes can be formed by solvent casting. The membranes prepared with BGNP formulations presented increased stiffness and showed acceptable extensibility in wet conditions without premature degradation. Also, it was noted that the magnesium-doped BGNPs increased the hydrophilicity of the composites when correlated with nanocomposites filled with non-doped BGNPs, indicating that changes in the formulation of the BGNPs could tailor the features of the nanocomposite. Importantly, upon immersion in SBF, the composite membranes induced apatite deposition compared with pure CHT membranes. Following this subject, Caridade *et al.* observed the biomineralization of CHT/BGNPs composite membranes by dynamical mechanical analysis (DMA).[52] The nanostructured membranes showed an improvement in the Young's modulus associated with the onset of apatite formation. Thus, the membranes had improved mechanical properties and higher bioactivity than both bare CHT membranes and CHT membranes containing bioactive glass microparticles.[52] Studies with osteoblastic-like cells (SaOs-2) revealed that the nanocomposite membranes were non-cytotoxic. It was further observed that the addition of BGNPs improved the proliferation and metabolism of human periodontal ligament cells (hPDLCs) and hBMSCs. Further, BGNPs promoted greater cell matrix mineralization by both types of cells.[90,99,127] Also regarding membranes, Luz *et al.* used a micro-imprinting strategy to create BGNP micropatterns onto CHT membranes.[128] The bioactive character of the BGNP spots allowed restricted nucleation and growth of apatite. The results showed that the fibroblast L929 cells mirrored the first bioactive pattern, choosing the milieu formed by the BGNPs rather than moving to the exposed CHT regions. With this strategy, it was found that it is feasible to spatially control the bioactive behavior and cellular interactions in a polymeric matrix. This method may be employed under co-cultures or to produce substrates that may confine cells in particular regions.[128]

In addition to hydrogels and membranes, further CHT nanocomposite scaffolds containing BGNPs have been built by freeze-drying.[129,130] These nanocomposites showed acceptable swelling and degradation. *In vitro* studies showed apatite deposition at the surface of the nanocomposite scaffolds, demonstrating their bioactive abilities. The study of the behavior of MG-63 cells revealed that cells adhered to the pore walls of the scaffolds and presented early indications of spreading. A particular aspect of CHT scaffolds is their shape memory capacity. Shape memory polymers can be distorted and locked into a temporary shape, which remains stationary unless presented with a stimulus that prompts the polymer to restore its primitive shape. Therefore, spherical nanocomposite scaffolds were produced to combine the shape memory properties of CHT and the biomineralization ability of BGNPs.[131,132] Adding BGNPs improved the bioactivity of the nanocomposite scaffold, as perceived by the precipitation of an apatite layer upon immersion in SBF; this demonstrates their osteoconductive potential. Further, including BGNPs in the CHT matrix improved the stiffness of the constructs. CHT/BGNPs composites showed superior shape memory properties compared to CHT, and the scaffold composites presented excellent shape memory properties, as outlined by their significant recovery ratios and high fixity ratios. The applicability of these structures was shown by proper geometric accommodation of previously compressed nanocomposites in a bone deformity. The natural shape memory behavior of these nanocomposites revealed their potential use for minimally invasive strategies in bone tissue therapies.[131,132]

Collagen

The application of collagen-based biomaterials in regenerative medicine has been growing intensely over the past few decades. Collagen plays a vital function in the organization of tissues and organs and assists in functional expressions of cells. Notably, type I collagen is the principal organic component of the bone matrix and is one of the most commonly used biomaterials.[133]

The angiogenic capacity of collagen nanocomposites containing BGNPs using the quail chorioallantoic membrane (CAM) was examined as a substitute for the classical mammalian models of angiogenesis (Fig. 3D).[10] Interestingly, at 24 h post-implantation, collagen films with 10 wt% of BGNPs stimulated angiogenesis by expanding the fraction of blood vessel branch points by 40%. In contrast, nanocomposite films containing 20 wt% BGNPs were found to suppress angiogenesis. This exploratory investigation revealed that supplementing a particular concentration of BGNPs in collagen films leads to an early angiogenic response.[10]

To circumvent the poor mechanical properties of collagen hydrogels in hard tissue engineering, El-Fiqi *et al.* developed nanocomposite hydrogels made of collagen and BGNPs functionalized with amine groups on their surfaces. The amine-functionalized BGNPs facilitated chemical bonding with amino acid sequences of the collagen molecules. Thus, the nanocomposite hydrogels exhibited improved physicochemical and mechanical stability due to physical crosslinking. Moreover, the hydrolytic and enzymatic degradation of the nanocomposite was diminished. MSCs cultivated within the nanocomposite hydrogels remained viable, with enhanced cytoskeletal extensions. Moreover, the addition of amine-functionalized BGNPs resulted in no noticeable shrinkage over 21 days.[134]

Gelatin

Due to concerns about the antigenicity associated with collagen, gelatin has attracted the attention of researchers.[135] Gelatin is a denatured protein that is extracted by hydrolysis of animal collagen; it has been widely used in foods, cosmetics, pharmaceutics, and medicine as wound dressings, as adhesives and absorbents for surgical use.[136]

In this regard, Koudehi *et al.* designed a BGNPs/gelatin conduit for peripheral nerve regeneration (Fig. 3E).[22] The guidance channel was examined in the right sciatic nerve of a male Wistar rat. Twenty rats were randomly divided into two experimental groups, one with the nanocomposite and the other comprising normal rats. The results showed that after three months, nerve regeneration of the nanocomposite group was statistically equivalent to the standard group. These results suggested that the nanocomposite could be suitable as a biocompatible and biodegradable candidate for peripheral nerve repair. The bone regeneration ability of the BGNPs/gelatin scaffold was also tested in a bone critical-sized defect.[137] The radiographic evaluation showed that the nanocomposite scaffolds could successfully bridge the critical-sized defect. X-ray analysis also revealed that bioactive glass scaffolds supported healthy bone formation by intramembranous formation. This study presents the development of nanocomposite scaffolds that contribute significantly to growth and healing of bone.[137]

Johari *et al.* evaluated the biocompatibility and regenerative properties of BGNPs in a gelatin scaffold by animal implantation using a rat model.[138] They showed that the nanocomposite was cell-compatible, as it allowed osteoblasts to adhere, spread and proliferate. The *in vivo* results indicated that the nanocomposite contributed to bone regeneration and was biodegradable and biocompatible. Moreover, the seeded scaffolds with osteoblasts enhanced the repair of critical bone defects.[138]

Wang *et al.* also combined BGNPs of different sizes with gelatin, forming nanocomposite scaffolds for artificial bone grafting.[139] They found that the mechanical properties of the nanocomposite scaffolds could match those of natural cancellous bones. Additionally, the size of BGNPs has been shown to have a substantial impact on the mechanical properties of nanoparticle–gelatin composite scaffolds. As the size of the BGNPs decreased, both the modulus and strength were found to increase, which probably resulted from the increasing interfacial area between the nanoparticles and the gelatin. This effect was also attributed to the homogeneous dispersion of the nanoparticles inside the polymer matrix and the active interactions between the particles and gelatin due to the surface silanol groups present on the surface of the nanoparticles. The bioactivity was also found to increase with decreasing BGNP size. Furthermore, the incorporation of BGNPs endowed the nanocomposite scaffolds with bioactivity, thus stimulating the attachment, growth, and proliferation of preosteoblasts.[139]

Gellan gum

Composites have been developed to demonstrate the possibility of enhancing the mechanical properties and the bioactivity of gellan gum using BGNPs (Fig. 3F).[24] Although the BGNPs agglomerated within the gellan gum matrix, they significantly improved the microstructure of the original gellan gum hydrogels as they increased the roughness of the pore walls, which may help cell attachment. Although the Young's modulus and the point of failure occurred at higher loads when gellan gum was reinforced, their mechanical properties were below the values for load-bearing applications. However, refinement of the mechanical properties could be achieved by a fine dispersion of the nanoparticles in the polymer matrix. Nevertheless, by including the BGNPs, the composite material could form an apatite layer when immersed in SBF. Further, the ADSCs remained viable and could adhere and spread within the produced sponge-like nanocomposite, which is a meaningful outcome regarding their application in bone tissue engineering.[24]

Gelatin/chitosan

Peter *et al.* introduced ternary BGNPs into a gelatin–CHT matrix which formed porous composite scaffolds upon freeze-drying.[140] They noted that the addition of BGNPs decreased the degradation and swelling ability of the scaffolds and increased protein adsorption. Biomineralization studies showed a higher number of mineral deposits on the nanocomposite scaffold, which increased with incubation time in SBF. Cell studies with human osteosarcoma cell line (MG-63) cells revealed that the composite scaffolds with BGNPs favored cell attachment and spreading. Therefore, the developed nanocomposite scaffold is a potential candidate for periodontal/alveolar bone tissue applications.[140]

Alginate dialdehyde/gelatin

The combination of gelatin and alginate dialdehyde (ADA–GEL) aims to overcome the limits of alginate, such as low viscosity and dissolution in physiological media. Most importantly, alginate discourages cell interactions that are essential features in tissue engineering. Therefore, ADA–GEL has been shown to support cell adhesion and proliferation.

Rottensteiner *et al.* combined ADA–GEL with quaternary BGNPs to produce hydrogel films by solvent casting.[141] *In vivo* implantation did not show a significant immune reaction and showed degradation of the films after four weeks, which would ideally address the onset of bone formation. Moreover, continuing vascularization could be detected after four weeks. However, no difference was noted between the composite and the pure ADA–GEL.[141]

In other work, ADA–GEL constructs incorporating BGNPs were produced by biofabrication to obtain a grid-like nanocomposite for bone tissue engineering purposes (Fig. 3G).[26] The BGNPs were synthesized from a sol–gel route and doped with strontium. This nanocomposite hydrogel successfully induced the formation of an apatite bone-like layer on its surface and could sustainably release a drug model. The biofabrication process allowed the incorporation of MG-63 cells into the composite material. Cells were homogeneously distributed within the hydrogel composite, and no difference was found in cell viability between plain ADA–GEL and the nanocomposite constructs, proving that the addition of BGNPs did not influence cell fate.[26]

These studies show that the addition of BGNPs may contribute to the bioactivity of ADA–GEL while preserving its advantages.

Gelatin/hyaluronic acid

Gelatin has been used to increase the flexibility of biomaterials; however, it has poor mechanical properties, particularly inadequate wet tensile strength. This feature is important because

gelatin or collagen devices are often designed to provide space-filling functions in aqueous environments.

In this regard, Zhou *et al.* studied the influence of BGNP content on the physicochemical and biological properties of Gel–HA/BGNPs composite scaffolds fabricated by freeze-drying. The authors could control the porosity and swelling by adjusting the BGNP content. Moreover, the addition of BGNPs strengthened the material and enhanced the viability and ALP activity of fibroblasts.

Collagen, hyaluronic acid, and phosphatidylserine

Wang *et al.* produced a novel porous bioactive nanocomposite composed of sol–gel-derived BGNPs, collagen, hyaluronic acid, and phosphatidylserine (BGNPs–COL–HYA–PS) by freeze-drying (Fig. 3H).[27] They further synthesized a cross-linked bioactive nanocomposite using 1-ethyl-3-(3-dimethylaminopropyl)carbodiimide and *N*-hydroxysuccinimide (EDC/NHS-cross-linked BGNPs–COL–HYA–PS). The biomineralization, degradation, and mechanical strength of the cross-linked composite scaffolds were superior to those of scaffolds without crosslinking. Further *in vitro* cell culture studies reported that MC3T3 cells adhered and spread on the surface of cross-linked BGNPs–COL–HYA–PS scaffolds, showing the biocompatibility of the nanocomposite.[27]

Following this work, Xie *et al.* studied the *in vivo* bone regeneration ability of EDC/NHS-cross-linked BGNPs–COL–HYA–PS composite scaffolds utilizing a rabbit radius defect model.[146] X-ray and histological studies confirmed the bone regeneration ability for plain nanocomposites and nanocomposites combined with growth factors. The bone defect was covered with new bone only in the nanocomposites grafted with BMP at eight weeks. Also, the nanocomposite combined with BMP showed improved ectopic bone formation compared with the composites without BMP.[146]

Gelatin/collagen

Barabadi *et al.* designed a scaffold for myocardial tissue engineering based on a blend of gelatin and collagen combined with BGNPs. They demonstrated that the incorporation of BGNPs into the hydrogel scaffold enhanced the differentiation of human endometrial stromal cells into the endothelial lineage and increased vascular endothelial growth factor expression, suggesting a beneficial role of BGNPs for angiogenesis in myocardial tissue engineering.[147] The finding suggested that BGNPs can also be considered for use in myocardial regeneration.

Conclusions

Regenerative medicine concepts in combination with material science/technology have produced new high-performance biomaterials for tissue regeneration. BGNPs and nanocomposites have undergone considerable developments, particularly in their synthesis, processing, and structural characterization, to understand their interactions with cells and their applications in tissue engineering. Also, BGNPs have been found to improve and direct the proliferation and differentiation of odontoblasts, cementoblasts, osteoblasts and fibroblasts. Although many studies have been performed to restore tissues using nanoscale bioactive glasses, these efforts are still mainly confined to laboratory studies. Also, the conjugation of nanostructured biomaterials with stem cells and growth factors to achieve the desired goal of tissue regeneration is showing promising results; however, more research is needed, especially in soft tissue reconstruction.

Significant progress is similarly being made to introduce nanoscale bioactive glass as fillers in polymers, to use their different material properties synergistically, and to stimulate tissue regeneration. An ongoing area of considerable investigation is the reproduction of nanosize features in biomaterials to resemble specific ECM structures to enhance the biological roles of existing polymeric biomaterials. Systems that integrate macroscale shapes, microscale pores and nanoscale architectures have been rapidly designed to optimize the function of biomaterials. However, further exploration is needed to exploit the novel features of these nanocomposites to address the challenges of hard and soft tissue regeneration.

Promising research fields are the incorporation of biomolecules, such as growth factors, and the controlled patterning of BGNPs within the polymeric matrix. This would provide exceptional control and tailoring of the mechanical and biological properties of the nanocomposite materials.

Further improvement in new nanoscale bioactive glasses and their combination with polymers and bioactive molecules may provide biomimetic materials that meet the challenges of hard and soft tissue engineering applications.

Acknowledgements

Álvaro J. Leite acknowledges the Portuguese Foundation for Science and Technology (FCT) for his doctoral grant (SFRH/BD/73174/2010).

References

1 S. Srinivasan, R. Jayasree, K. P. Chennazhi, S. V. Nair and R. Jayakumar, *Carbohydr. Polym.*, 2012, **87**, 274–283.
2 T. J. Brunner, R. N. Grass and W. J. Stark, *Chem. Commun.*, 2006, 1384–1386, DOI: 10.1039/B517501A,.
3 J. R. Jones, *Acta Biomater.*, 2013, **9**, 4457–4486.
4 M. Peter, P. T. S. Kumar, N. S. Binulal, S. V. Nair, H. Tamura and R. Jayakumar, *Carbohydr. Polym.*, 2009, **78**, 926–931.
5 M. B. Oliveira, G. M. Luz and J. F. Mano, *J. Mater. Chem. B*, 2014, **2**, 5627–5638.
6 M. D. Shoulders and R. T. Raines, *Annu. Rev. Biochem.*, 2009, **78**, 929–958.
7 N. R. Zhao, Y. J. Wang, X. F. Chen, Y. X. Yang, K. Wei and G. Wu, *Asbm6: Advanced Biomaterials VI*, 2005, **288-289**, 179–182.
8 L. L. Hench, *Am. Ceram. Soc. Bull.*, 1993, **72**, 93–98.
9 Z. K. Hong, R. L. Reis and J. F. Mano, *Acta Biomater.*, 2008, **4**, 1297–1306.
10 G. E. Vargas, L. A. Haro Durand, V. Cadena, M. Romero, R. V. Mesones, M. Mačković, S. Spallek, E. Spiecker,

A. R. Boccaccini and A. A. Gorustovich, *J. Mater. Sci.: Mater. Med.*, 2013, **24**, 1261–1269.
11 C. Mao, X. Chen, G. Miao and C. Lin, *Biomed. Mater.*, 2015, **10**, 025005.
12 A. A. Gorustovich, J. A. Roether and A. R. Boccaccini, *Tissue Eng., Part B*, 2009, **16**, 199–207.
13 Z. K. Hong, G. M. Luz, P. J. Hampel, M. S. Jin, A. X. Liu, X. S. Chen and J. F. Mano, *J. Biomed. Mater. Res., Part A*, 2010, **95A**, 747–754.
14 Z. Hong, G. M. Luz, P. J. Hampel, M. Jin, A. Liu, X. Chen and J. F. Mano, *J. Biomed. Mater. Res., Part A*, 2010, **95**, 747–754.
15 S. M. Amit, S. Xinfeng and G. M. Antonios, *Tissue Engineering and Artificial Organs*, CRC Press, 2006, pp. 40–41, DOI: 10.1201/9781420003871.ch40.
16 E. Engel, A. Michiardi, M. Navarro, D. Lacroix and J. A. Planell, *Trends Biotechnol.*, 2008, **26**, 39–47.
17 C. T. Laurencin, S. G. Kumbar and S. P. Nukavarapu, *Wiley Interdiscip. Rev.: Nanomed. Nanobiotechnol.*, 2009, **1**, 6–10.
18 G. Wei and P. X. Ma, *Adv. Funct. Mater.*, 2008, **18**, 3566–3582.
19 N. M. Alves, I. Pashkuleva, R. L. Reis and J. F. Mano, *Small*, 2010, **6**, 2208–2220.
20 L. Zhang and T. J. Webster, *Nano Today*, 2009, **4**, 66–80.
21 T. J. Webster, C. Ergun, R. H. Doremus, R. W. Siegel and R. Bizios, *Biomaterials*, 2000, **21**, 1803–1810.
22 M. F. Koudehi, A. A. I. Fooladi, K. Mansoori, Z. Jamalpoor, A. Amiri and M. R. Nourani, *J. Mater. Sci.: Mater. Med.*, 2014, **25**, 363–373.
23 A. Pandit and D. I. Zeugolis, *Nanomedicine*, 2016, **11**, 985–987.
24 A. Gantar, L. P. da Silva, J. M. Oliveira, A. P. Marques, V. M. Correlo, S. Novak and R. L. Reis, *Mater. Sci. Eng., C*, 2014, **43**, 27–36.
25 G. M. Luz and J. F. Mano, *Philos. Trans. R. Soc., A*, 2009, **367**, 1587–1605.
26 A. J. Leite, B. Sarker, T. Zehnder, R. Silva, J. F. Mano and A. R. Boccaccini, *Eur. Cells Mater.*, 2016, **31**(suppl. 1), 468.
27 Y. J. Wang, C. R. Yang, X. F. Chen and N. R. Zhao, *Macromol. Mater. Eng.*, 2006, **291**, 254–262.
28 J. F. Mano, G. A. Silva, H. S. Azevedo, P. B. Malafaya, R. A. Sousa, S. S. Silva, L. F. Boesel, J. M. Oliveira, T. C. Santos, A. P. Marques, N. M. Neves and R. L. Reis, *J. R. Soc., Interface*, 2007, **4**, 999–1030.
29 P. Saravanapavan, J. R. Jones, R. S. Pryce and L. L. Hench, *J. Biomed. Mater. Res., Part A*, 2003, **66A**, 110–119.
30 R. L. Siqueira, O. Peitl and E. D. Zanotto, *Mater. Sci. Eng., C*, 2011, **31**, 983–991.
31 A. R. Boccaccini, M. Erol, W. J. Stark, D. Mohn, Z. K. Hong and J. F. Mano, *Compos. Sci. Technol.*, 2010, **70**, 1764–1776.
32 T. J. Brunner, W. J. Stark and A. R. Boccaccini, *Nanotechnologies for the Life Sciences*, Wiley-VCH Verlag GmbH & Co. KGaA, 2007, DOI: 10.1002/9783527610419.ntls0142.
33 S. Loher, W. J. Stark, M. Maciejewski, A. Baiker, S. E. Pratsinis, D. Reichardt, F. Maspero, F. Krumeich and D. Günther, *Chem. Mater.*, 2005, **17**, 36–42.
34 W. Stöber, A. Fink and E. Bohn, *J. Colloid Interface Sci.*, 1968, **26**, 62–69.
35 I. Elgayar, A. E. Aliev, A. R. Boccaccini and R. G. Hill, *J. Non-Cryst. Solids*, 2005, **351**, 173–183.
36 G. M. Luz and J. F. Mano, *J. Nanopart. Res.*, 2013, **15**, 1–11.
37 A. Lukowiak, J. Lao, J. Lacroix and J.-M. Nedelec, *Chem. Commun.*, 2013, **49**, 6620–6622.
38 Z. Hong, A. Liu, L. Chen, X. Chen and X. Jing, *J. Non-Cryst. Solids*, 2009, **355**, 368–372.
39 W. Xia and J. Chang, *Mater. Lett.*, 2007, **61**, 3251–3253.
40 G. M. Luz and J. F. Mano, *Nanotechnology*, 2011, **22**, 494014.
41 G. M. Luz, Á. J. Leite, A. I. Neto, W. Song and J. F. Mano, *Mater. Lett.*, 2011, **65**, 296–299.
42 O. Tsigkou, S. Labbaf, M. M. Stevens, A. E. Porter and J. R. Jones, *Adv. Healthcare Mater.*, 2014, **3**, 115–125.
43 X. F. Chen, B. Lei, Y. J. Wang and N. Zhao, *J. Non-Cryst. Solids*, 2009, **355**, 791–796.
44 Q. Liang, Q. Hu, G. Miao, B. Yuan and X. Chen, *Mater. Lett.*, 2015, **148**, 45–49.
45 B. Lei, X. Chen, X. Han and J. Zhou, *J. Mater. Chem.*, 2012, **22**, 16906–16913.
46 K. W. Powers, M. Palazuelos, B. M. Moudgil and S. M. Roberts, *Nanotoxicology*, 2007, **1**, 42–51.
47 L. C. Gerhardt, K. L. Widdows, M. M. Erol, C. W. Burch, J. A. Sanz-Herrera, I. Ochoa, R. Staempfli, I. S. Roqan, S. Gabe, T. Ansari and A. R. Boccaccini, *Biomaterials*, 2011, **32**, 4096–4108.
48 S. M. Carvalho, A. A. R. Oliveira, C. A. Jardim, C. B. S. Melo, D. A. Gomes, M. de Fátima Leite and M. M. Pereira, *J. Tissue Eng. Regener. Med.*, 2012, **6**, 813–821.
49 M. Vollenweider, T. J. Brunner, S. Knecht, R. N. Grass, M. Zehnder, T. Imfeld and W. J. Stark, *Acta Biomater.*, 2007, **3**, 936–943.
50 G. Mendonça, D. B. S. Mendonça, F. J. L. Aragão and L. F. Cooper, *Biomaterials*, 2008, **29**, 3822–3835.
51 E. Palin, H. N. Liu and T. J. Webster, *Nanotechnology*, 2005, **16**, 1828–1835.
52 S. G. Caridade, E. G. Merino, N. M. Alves, V. d. Z. Bermudez, A. R. Boccaccini and J. F. Mano, *J. Mech. Behav. Biomed. Mater.*, 2013, **20**, 173–183.
53 S. Liu, W. Gong, Y. Dong, Q. Hu, X. Chen and X. Gao, *RSC Adv.*, 2015, **5**, 38830–38836.
54 W. Y. Gong, Y. M. Dong, X. F. Chen and B. Karabucak, *Chin. J. Dent. Res.*, 2012, **15**, 145–152.
55 J. Ajita, S. Saravanan and N. Selvamurugan, *Mater. Sci. Eng., C*, 2015, **53**, 142–149.
56 J. A. Champion and S. Mitragotri, *Proc. Natl. Acad. Sci. U. S. A.*, 2006, **103**, 4930–4934.
57 Y. Geng, P. Dalhaimer, S. Cai, R. Tsai, M. Tewari, T. Minko and D. E. Discher, *Nat. Nano*, 2007, **2**, 249–255.
58 R. Colquhoun and K. E. Tanner, *Biomed. Mater.*, 2016, **11**, 014105.
59 Z. Hong, E. G. Merino, R. L. Reis and J. F. Mano, *Adv. Eng. Mater.*, 2009, **11**, B25–B29.
60 Y. Li, X. Chen, C. Ning, B. Yuan and Q. Hu, *Mater. Lett.*, 2015, **161**, 605–608.

61 F.-Z. Cui and J. Ge, *J. Tissue Eng. Regener. Med.*, 2007, **1**, 185–191.
62 X. Chen, C. Guo and N. Zhao, *Appl. Surf. Sci.*, 2008, **255**, 466–468.
63 J.-H. Lee, M.-S. Kang, C. Mahapatra and H.-W. Kim, *PLoS One*, 2016, **11**, e0150727.
64 X. Yan, C. Yu, X. Zhou, J. Tang and D. Zhao, *Angew. Chem., Int. Ed.*, 2004, **43**, 5980–5984.
65 X. Li, X. Chen, G. Miao, H. Liu, C. Mao, G. Yuan, Q. Liang, X. Shen, C. Ning and X. Fu, *J. Mater. Chem. B*, 2014, **2**, 7045–7054.
66 N. Z. Knezevic and J.-O. Durand, *Nanoscale*, 2015, **7**, 2199–2209.
67 T.-H. Kim, R. K. Singh, M. S. Kang, J.-H. Kim and H.-W. Kim, *Nanoscale*, 2016, **8**, 8300–8311.
68 W. Xiaojian and L. Wei, *Nanotechnology*, 2016, **27**, 225102.
69 A. Hoppe, N. S. Güldal and A. R. Boccaccini, *Biomaterials*, 2011, **32**, 2757–2774.
70 M. N. Rahaman, D. E. Day, B. Sonny Bal, Q. Fu, S. B. Jung, L. F. Bonewald and A. P. Tomsia, *Acta Biomater.*, 2011, **7**, 2355–2373.
71 R. Detsch, M. Rübner, P. L. Strissel, D. Mohn, E. Strasser, W. J. Stark, R. Strick and A. R. Boccaccini, *Nanomedicine*, 2016, **11**, 1093–1105.
72 A. Moorthi, P. R. Parihar, S. Saravanan, M. Vairamani and N. Selvamurugan, *Mater. Sci. Eng., C*, 2014, **43**, 458–464.
73 Y.-F. Goh, A. Z. Alshemary, M. Akram, M. R. A. Kadir and R. Hussain, *Int. J. Appl. Glass Sci.*, 2014, **5**, 255–266.
74 A. M. El-Kady, A. F. Ali, R. A. Rizk and M. M. Ahmed, *Ceram. Int.*, 2012, **38**, 177–188.
75 K. Kaur, K. J. Singh, V. Anand, H. Kaur and D. S. Arora, *AIP Conf. Proc.*, 2015, **1675**, 020020.
76 V. Rajendran, M. Prabhu and R. Suriyaprabha, *J. Mater. Sci.*, 2015, **50**, 5145–5156.
77 B. Pemmer, A. Roschger, A. Wastl, J. G. Hofstaetter, P. Wobrauschek, R. Simon, H. W. Thaler, P. Roschger, K. Klaushofer and C. Streli, *Bone*, 2013, **57**, 184–193.
78 H. Rico and L. F. Villa, *Calcif. Tissue Int.*, 2000, **67**, 422–423.
79 J. Zhang, Y.-D. Park, W.-J. Bae, A. El-Fiqi, S.-H. Shin, E.-J. Lee, H.-W. Kim and E.-C. Kim, *J. Biomater. Appl.*, 2015, **29**, 954–964.
80 L. A. Strobel, N. Hild, D. Mohn, W. J. Stark, A. Hoppe, U. Gbureck, R. E. Horch, U. Kneser and A. R. Boccaccini, *J. Nanopart. Res.*, 2013, **15**, 1–9.
81 A. Hoppe, B. Sarker, R. Detsch, N. Hild, D. Mohn, W. J. Stark and A. R. Boccaccini, *J. Non-Cryst. Solids*, 2014, **387**, 41–46.
82 Y. Xue, Y. Du, J. Yan, Z. Liu, P. X. Ma, X. Chen and B. Lei, *J. Mater. Chem. B*, 2015, **3**, 3831–3839.
83 S. Labbaf, O. Tsigkou, K. H. Müller, M. M. Stevens, A. E. Porter and J. R. Jones, *Biomaterials*, 2011, **32**, 1010–1018.
84 L. Ji, W. Wang, D. Jin, S. Zhou and X. Song, *Mater. Sci. Eng., C*, 2015, **46**, 1–9.
85 A. Doostmohammadi, A. Monshi, M. H. Fathi, R. Salehi, S. Karbasi, O. Braissant and A. U. Daniels, *Biocompatibility Evaluation of Bioglass Nanoparticles to Chondrocyte Cells by Isothermal Microcalorimetry*, 7th Iranian Conference of Biomedical Engineering (ICBME), 2010, pp. 1–4.
86 O. Agda Aline Rocha de, S. Dickson Alves de, D. Luisa Lima Silveira, C. Sandhra Maria de, M. Herman Sander and P. Marivalda de Magalhães, *Biomed. Mater.*, 2013, **8**, 025011.
87 M. Tavakoli, E. Bateni, M. Rismanchian, M. Fathi, A. Doostmohammadi, A. Rabiei, H. Sadeghi, M. Etebari and M. Mirian, *Dent. Res. J.*, 2012, **9**, 314–320.
88 M. Rismanchian, N. Khodaeian, L. Bahramian, M. Fathi and H. Sadeghi-Aliabadi, *Iran. J. Pharm. Res.*, 2013, **12**, 437–443.
89 A. L. Carvalho, A. C. Vale, M. P. Sousa, A. M. Barbosa, E. Torrado, J. F. Mano and N. M. Alves, *J. Mater. Chem. B*, 2016, **4**, 5385–5393.
90 G. M. Luz and J. F. Mano, *Biomed. Mater.*, 2012, **7**, 054104.
91 H. Hajiali, M. Hosseinalipour, S. Karbasi and M. A. Shokrgozar, *Int. J. Artif. Organs*, 2012, **35**, 1015–1024.
92 A. J. Leite, B. Sarker, T. Zehnder, R. Silva, J. F. Mano and A. R. Boccaccini, *Biofabrication*, 2016, **8**, 035005.
93 P. Naruphontjirakul, L. Greasley Sarah, S. Chen, E. Porter Alexandra and R. Jones Julian, *Biomed. Glasses*, 2016, **2**, 72–81.
94 M. Mačković, A. Hoppe, R. Detsch, D. Mohn, W. J. Stark, E. Spiecker and A. R. Boccaccini, *J. Nanopart. Res.*, 2012, **14**, 1–22.
95 H. Wang, X. Chen, Y. Wang and D. Cheng, *J. Wuhan Univ. Technol., Mater. Sci. Ed.*, 2013, **28**, 1053–1057.
96 N. M. Alves, I. B. Leonor, H. S. Azevedo, R. L. Reis and J. F. Mano, *J. Mater. Chem.*, 2010, **20**, 2911–2921.
97 K. Rezwan, Q. Z. Chen, J. J. Blaker and A. R. Boccaccini, *Biomaterials*, 2006, **27**, 3413–3431.
98 V. Guarino, F. Causa and L. Ambrosio, *Expert Rev. Med. Devices*, 2007, **4**, 405–418.
99 G. M. Luz and J. F. Mano, *Advanced Materials Forum V, Pt 1 and 2*, 2010, **636-637**, 31–35.
100 A. Liu, Z. Hong, X. Zhuang, X. Chen, Y. Cui, Y. Liu and X. Jing, *Acta Biomater.*, 2008, **4**, 1005–1015.
101 D. Couto, Z. Hong and J. Mano, *Acta Biomater.*, 2009, **5**, 115–123.
102 S. K. Misra, D. Mohn, T. J. Brunner, W. J. Stark, S. E. Philip, I. Roy, V. Salih, J. C. Knowles and A. R. Boccaccini, *Biomaterials*, 2008, **29**, 1750–1761.
103 Q. Z. Z. Chen, I. D. Thompson and A. R. Boccaccini, *Biomaterials*, 2006, **27**, 2414–2425.
104 F. Baino and C. Vitale-Brovarone, *J. Biomed. Mater. Res., Part A*, 2011, **97A**, 514–535.
105 Z. Zhou, S. He, B. Ou, T. Huang, W. Zeng, L. Liu, Q. Liu, J. Chen, Y. Zhao, Z. Yang and D. Cao, *J. Macromol. Sci., Part B: Phys.*, 2014, **53**, 1145–1155.
106 Z. Hong, R. L. Reis and J. F. Mano, *J. Biomed. Mater. Res., Part A*, 2009, **88A**, 304–313.
107 S. K. Misra, S. P. Valappil, I. Roy and A. R. Boccaccini, *Biomacromolecules*, 2006, **7**, 2249–2258.
108 J. Rodenas-Rochina, J. L. Gomez Ribelles and M. Lebourg, *J. Mater. Sci.: Mater. Med.*, 2013, **24**, 1293–1308.

109 N. Hild, P. N. Tawakoli, J. G. Halter, B. Sauer, W. Buchalla, W. J. Stark and D. Mohn, *Acta Biomater.*, 2013, **9**, 9118–9125.

110 E. Tamjid, R. Bagheri, M. Vossoughi and A. Simchi, *Mater. Sci. Eng., C*, 2011, **31**, 1526–1533.

111 G. Zhao, A. L. Raines, M. Wieland, Z. Schwartz and B. D. Boyan, *Biomaterials*, 2007, **28**, 2821–2829.

112 T. J. Webster, R. W. Siegel and R. Bizios, *Biomaterials*, 1999, **20**, 1221–1227.

113 J. F. Mano, *Biomimetic Approaches for Biomaterials Development*, Wiley, 2013.

114 H. Ylänen, *Bioactive Glasses: Materials, Properties and Applications*, Elsevier Science, 2011.

115 P. de Vos, M. M. Faas, M. Spasojevic and J. Sikkema, *Int. Dairy J.*, 2010, **20**, 292–302.

116 K. Y. Lee and D. J. Mooney, *Prog. Polym. Sci.*, 2012, **37**, 106–126.

117 J. P. Cattalini, J. García, A. R. Boccaccini, S. Lucangioli and V. Mouriño, *Procedia Eng.*, 2013, **59**, 78–84.

118 P. C. Juan, R. Judith, H. Alexander, P. Fatemeh, D. Luis Haro, G. Alejandro, R. B. Aldo, L. Silvia and M. Viviana, *Biomed. Mater.*, 2016, **11**, 065003.

119 V. Mourino, P. Newby, F. Pishbin, J. P. Cattalini, S. Lucangioli and A. R. Boccaccini, *Soft Matter*, 2011, **7**, 6705–6712.

120 J. P. Cattalini, A. Hoppe, F. Pishbin, J. Roether, A. R. Boccaccini, S. Lucangioli and V. Mouriño, *J. R. Soc., Interface*, 2015, **12**, 20150509.

121 T. H. Silva, A. Alves, B. M. Ferreira, J. M. Oliveira, L. L. Reys, R. J. F. Ferreira, R. A. Sousa, S. S. Silva, J. F. Mano and R. L. Reis, *Int. Mater. Rev.*, 2012, **57**, 276–306.

122 S. Patel and A. Goyal, *Int. J. Biol. Macromol.*, 2017, **97**, 331–338.

123 S. Sowmya, P. T. S. Kumar, K. P. Chennazhi, S. V. Nair, H. Tamura and R. Jayakumar, *Trends in Biomaterials and Artificial Organs*, 2011, **25**, 1–11.

124 R. C. F. Cheung, T. B. Ng, J. H. Wong and W. Y. Chan, *Mar. Drugs*, 2015, **13**, 5156–5186.

125 S. Kalia and L. Avérous, *Biopolymers: Biomedical and Environmental Applications*, Wiley, 2011.

126 M. Wieckiewicz, K. W. Boening, N. Grychowska and A. Paradowska-Stolarz, *Mini-Rev. Med. Chem.*, 2017, **17**, 401–409.

127 J. Mota, N. Yu, S. G. Caridade, G. M. Luz, M. E. Gomes, R. L. Reis, J. A. Jansen, X. F. Walboomers and J. F. Mano, *Acta Biomater.*, 2012, **8**, 4173–4180.

128 G. M. Luz, L. Boesel, A. del Campo and J. F. Mano, *Langmuir*, 2012, **28**, 6970–6977.

129 M. Peter, N. S. Binulal, S. Soumya, S. V. Nair, T. Furuike, H. Tamura and R. Jayakumar, *Carbohydr. Polym.*, 2010, **79**, 284–289.

130 M. Pourhaghgouy, A. Zamanian, M. Shahrezaee and M. P. Masouleh, *Mater. Sci. Eng., C*, 2016, **58**, 180–186.

131 Á. J. Leite, S. G. Caridade and J. F. Mano, *J. Non-Cryst. Solids*, 2016, **432**(part A), 158–166.

132 C. O. Correia, Á. J. Leite and J. F. Mano, *Carbohydr. Polym.*, 2015, **123**, 39–45.

133 C. H. Lee, A. Singla and Y. Lee, *Int. J. Pharm.*, 2001, **221**, 1–22.

134 A. El-Fiqi, J. H. Lee, E.-J. Lee and H.-W. Kim, *Acta Biomater.*, 2013, **9**, 9508–9521.

135 W. A. Starin, *J. Infect. Dis.*, 1918, **23**, 139–158.

136 S.-h. Hsu, K.-C. Hung and C.-W. Chen, *J. Mater. Chem. B*, 2016, **4**, 7493–7505.

137 F. Hafezi, F. Hosseinnejad, A. A. I. Fooladi, S. M. Mafi, A. Amiri and M. R. Nourani, *J. Mater. Sci.: Mater. Med.*, 2012, **23**, 2783–2792.

138 B. Johari, M. Kadivar, S. Lak, M. Gholipourmalekabadi, A. M. Urbanska, M. Mozafari, M. Ahmadzadehzarajabad, A. Azarnezhad, S. Afshari, J. Zargan and S. Kargozar, *Int. J. Artif. Organs*, 2016, **39**, 524.

139 C. Wang, H. Shen, Y. Tian, Y. Xie, A. Li, L. Ji, Z. Niu, D. Wu and D. Qiu, *ACS Appl. Mater. Interfaces*, 2014, **6**, 13061–13068.

140 M. Peter, N. S. Binulal, S. V. Nair, N. Selvamurugan, H. Tamura and R. Jayakumar, *Chem. Eng. J.*, 2010, **158**, 353–361.

141 U. Rottensteiner, B. Sarker, D. Heusinger, D. Dafinova, S. N. Rath, J. P. Beier, U. Kneser, R. E. Horch, R. Detsch, A. R. Boccaccini and A. Arkudas, *Materials*, 2014, **7**, 1957–1974.

142 D. S. Couto, N. M. Alves and J. F. Mano, *J. Nanosci. Nanotechnol.*, 2009, **9**, 1741–1748.

143 S. J. Rego, A. C. Vale, G. M. Luz, J. F. Mano and N. M. Alves, *Langmuir*, 2016, **32**, 560–568.

144 J. R. Rodrigues, N. M. Alves and J. F. Mano, *RSC Adv.*, 2016, **6**, 75988–75999.

145 H. W. Kim, J. H. Song and H. E. Kim, *J. Biomed. Mater. Res., Part A*, 2006, **79A**, 698–705.

146 E. Xie, Y. Y. Hu, X. F. Chen, J. P. Bai, L. Ren and Z. Zhang, *2008 3rd IEEE International Conference on Nano/Micro Engineered and Molecular Systems*, 2008, vol. 1–3, pp. 943–946, DOI: 10.1109/NEMS.2008.4484477.

147 Z. Barabadi, M. Azami, E. Sharifi, R. Karimi, N. Lotfibakhshaiesh, R. Roozafzoon, M. T. Joghataei and J. Ai, *Mater. Sci. Eng., C*, 2016, **69**, 1137–1146.

